Automated Design of Pin-Constrained Digital Microfluidic Arrays for Lab-on-a-Chip Applications*

William L. Hwang, Fei Su, and Krishnendu Chakrabarty
Department of Electrical & Computer Engineering
Duke University, Durham, NC 27708, USA
{*wlh,fs,krish*}@ee.duke.edu

ABSTRACT

Microfluidics-based biochips, also referred to as lab-on-a-chip (LoC), are devices that integrate fluid-handling functions such as sample preparation, analysis, separation, and detection. This emerging technology combines electronics with biology to open new application areas such as point-of-care diagnosis, on-chip DNA analysis, and automated drug discovery. We propose a design automation method for pin-constrained LoCs that manipulate nanoliter volumes of discrete droplets on a microfluidic array. In contrast to the direct-addressing scheme that has been studied thus far in the literature, we assign a small number of independent control pins to a large number of electrodes in the LoC, thereby reducing design complexity and product cost. We apply the proposed method to a microfluidic array for a set of multiplexed bioassays.

Categories and Subject Descriptors

B.7.1 B.7.2 **[Integrated Circuits]**: Types and Design Styles, Design Aids.

General Terms: Algorithms, Performance, Design

Keywords

Pin-constrained design, virtual partitioning, microfluidic biochips.

1. INTRODUCTION

Biochips based on microfluidics technology are soon expected to offer miniaturization, automation and integration in the biochemical analysis laboratory. Microfluidic biochips, or lab-on-a-chip, are devices that integrate various fluid-handling functions, such as sample preparation, analysis, separation, and detection [1,2,3]. This emerging technology combines electronics with biology to open new areas of research and field applications, e.g., point-of-care diagnosis, on-chip DNA analysis, and drug screening [2,3].

A microfluidic lab-on-a-chip is based on the control of microliter and nanoliter volumes of liquids. Currently, most commercially-available microfluidic devices rely on continuous-flow in etched microchannels [1,4,5]. An alternative is to design systems that utilize droplets with microliter and nanoliter volumes. The droplets in such systems are actuated using electrical means, thereby obviating the need for cumbersome micropumps and microvalves. Droplet-based systems also offer reconfigurability and a scalable system architecture based on a two-dimensional array [6,7]. Droplet motion in such devices is typically controlled by a system clock, which is similar in operation to a digital microprocessor. Thus, this novel technology is referred to as "digital microfluidics".

* This research was supported by the National Science Foundation under grant numbers IIS-0312352 and CCF-0541055.

DAC 2006, July 24–28, 2006, San Francisco, California, USA.

The level of system integration and design complexity of such mixed-technology devices are expected to increase substantially, as more high-throughput bioassays are executed concurrently on the same platform [8]. Thus, biochip-specific design automation techniques are especially important for this emerging marketplace.

A digital microfluidic biochip typically consists of a two-dimensional patterned metal electrode array (e.g., chrome or indium tin oxide), on which droplets containing biological samples are dispensed, transported, mixed, incubated, separated or detected. Various addressing schemes can be used to activate individual cells in a microfluidic array. In direct-addressing schemes, each cell of the patterned electrodes can be accessed directly and independently via a dedicated control pin. Most design and CAD research for digital microfluidic biochips has been focused on such directly-addressable chips [10,11]. This method is suitable for small/medium-scale microfluidic electrode arrays (<10×10 electrodes). However, for emerging large-scale digital microfluidic biochips (>100×100 electrodes), multi-layer electrical connection structures and complicated routing solutions are required due to the large number of independent control pins (e.g., 10^4 pins for a 100×100 array). Product cost, however, is a major marketability driver due to the disposable nature of most emerging devices. Hence, simpler routing solutions are necessary.

Recently, multi-layer printed circuit board (PCB) technology has been proposed as a means to rapidly prototype and inexpensively mass-fabricate digital microfluidic biochips [12,15]. However, multiple metal layers for PCB design may lead to reliability problems and increase fabrication cost. Thus, reducing the number of independent control pins is important for its successful commercialization. In theory, we could maintain individual electrode addressing by employing a serial to parallel interface. However, this would require active elements that would increase chip cost.

We propose a new design automation method for pin-constrained digital microfluidic biochips. In contrast to the direct-addressing scheme, a small number of independent control pins are assigned to a large number of electrodes, thereby dramatically reducing the input bandwidth between the electronic controller and the microfluidic array. We evaluate the proposed method by applying it to an array used for multiplexed bioassays.

The organization of the rest of the paper is as follows. We first provide an overview of digital microfluidic biochips in Section 2. Some related prior work is discussed in Section 3. Next, Section 4 formulates the design problem for pin-constrained digital microfluidic arrays. In Section 5, we propose a virtual partitioning scheme to reduce interference for a pin-constrained array and evaluate it using a set of real-life bioassays. Finally, conclusions are drawn in Section 6.

2. DIGITAL MICROFLUIDIC BIOCHIPS

A digital microfluidic platform consists of two parallel plates, between which a droplet is sandwiched (Figure 1). The bottom plate contains a patterned array of control electrodes, and the top plate is coated with a continuous ground electrode. A droplet rests on a hydrophobic surface over an electrode that controls its wettability

through the application of an electric field. The actuation mechanism is based on the principle of electrowetting, i.e., interfacial tension gradients can be created to move the droplets to the charged electrode by switching the voltage applied across adjacent electrodes. By using the electrowetting phenomenon, droplets can be moved to any location on a two-dimensional array.

In addition to transport, fluid-handling operations such as merging, splitting, mixing, and dispensing of nano-liter droplets have been demonstrated in the same manner by varying the patterns of control voltage activation. For example, mixing can be performed by routing two droplets to the same location and then turning them about some pivot points [14]. Since the liquid is manipulated by software programming, these operations can be performed anywhere on the array. This is in contrast to continuous-flow systems, where the fluidic operations must be executed in specific micromixers or microchambers fixed on a substrate. This flexibility is referred to as the reconfigurability of digital microfluidic biochips. Droplet routes are programmed into a microcontroller that controls the voltages of electrodes in the array. In addition to the reconfigurable microfluidic array, optical detectors are also often integrated into digital microfluidic arrays to monitor colorimetric bioassays [3].

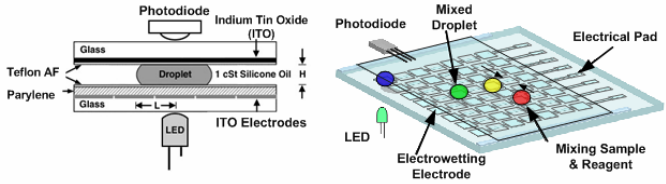

Figure 1. Schematic diagram of a digital microfluidic biochip.

3. RELATED PRIOR WORK

Research on design and CAD methodologies for digital microfluidic biochips has gained momentum in recent years. In [10], a system design methodology has been proposed to apply classical architectural-level synthesis techniques to the design of digital microfluidic biochips. The optimization problem of bioassay scheduling under resource constraints as well as the resource binding problem are studied. The problem of microfluidic module placement, where array area and fault tolerance serve as the placement criteria, is discussed in [11]. In [16], an integrated design framework is proposed to unify operation scheduling, resource binding, and module placement into one synthesis procedure. However, all these prior techniques assume that each electrode in the microfluidic array is individually and independently accessible; thus they require a very large number of control pins for large-scale biochips, which may lead to an unacceptably high overhead for commercial devices.

A problem related to pin-constrained design of digital microfluidic biochips has been analyzed in [3]. In order to minimize the number of electrical contacts, the fabricated electrowetting-based biochip uses a multi-phase bus for the fluidic pathways. In an *n*-phase bus, every *n*th electrode is electrically connected. Thus, only *n* control pins are needed for a transport bus, irrespective of the number of electrodes that it contains. Although the multi-phase bus method reduces the number of control pins, it is only applicable to one-dimensional arrays.

In other recent work, [17] presents a cross-reference driving scheme for digital microfluidic biochips, which allows control of an $n \times m$ grid array with only $n+m$ control pins. In this method, electrode rows are patterned on both the top and bottom plates, and placed orthogonally. In order to drive a droplet along the X-direction, electrode rows on the bottom plate serve as driving electrodes, while electrode rows on the top serve as reference ground electrodes [17]. The roles are reversed for movement along the Y-direction. This cross-reference method facilitates the reduction of control pins. However, it requires a special electrode structure (i.e., both top and bottom plates containing electrode rows), which results in increased manufacturing cost for disposable microfluidic chips. Moreover, this design is not suitable for high-throughput assays.

4. PIN ASSIGNMENT PROBLEM

In this section, we formulate the application-independent pin-constraint problem for a two-dimensional electrode array.

4.1 Minimum Number of Pins for Single Droplet

Given a two-dimensional microfluidic chip, the problem of determining the minimum number of independent control pins, k, necessary to have full control of a single droplet can be reduced to the well-known graph-coloring problem [18]. Full control means that a droplet can be moved to any cell on the array through an appropriate activation sequence.

While the problem of finding the chromatic number of a graph is NP-hard [19], it is trivial to observe that for rectangular arrays of size greater than 3x3, the largest number of directly adjacent neighbors to any cell is four. Hence, we set the number of independent control pins, $k \geq 5$, in order to guarantee that we can color each cell and all of its directly adjacent neighbors with different colors. We have experimentally verified that the diagonally adjacent neighbors have no effect on a droplet at a particular cell when the electrode size is sufficiently small. A possible pin layout using 5 pins for a 4x4 array is shown as an example in Figure 2. Note that increases in array size do not change the required number of independent pins for full control of a single droplet.

1	2	3	5
3	5	4	1
4	1	2	3
2	3	5	4

Figure 2. 5-pin layout for 4x4 array (entries are pin numbers).

4.2 Pin-Assignment Problem for Two Droplets

The interference constraints are designed to prevent "long-range" interference between the intended paths of droplets whereas the fluidic constraints are necessary to avoid "short-range" interference in the form of inadvertent mixing. This is because interference is a manifestation of control pin sharing between cells anywhere on the array while mixing (i.e., when fluidic constraints are violated) is a result of physical contact between droplets.

Ignoring the diagonal adjacent effect, the fluidic constraints verified experimentally in [20] can be expressed as:

$$(1)\ \{P_i(t+1)\} \cap N_j(t+1) = \varnothing;\ (2)\ \{P_i(t+1)\} \cap N_j(t) = \varnothing;\ (3)\ \{P_j(t+1)\} \cap N_j(t) = \varnothing$$

We first examine the interference problem for two droplets. For multiple droplets, the interference problem can be reduced to the two-droplet problem by examining all possible pairs of droplets. In general, any sequence of movements for multiple droplets can occur in parallel. We analyze interference between two droplets for a single clock cycle, during which time a droplet can only move to a directly adjacent cell. Any path can be decomposed into unit movements, and we say that the two paths are compatible iff all of their individual steps do not interfere.

In some situations, we would like both droplets to move to another cell in the next clock cycle. If this is not possible without interference, then a contingency plan is to have one droplet undergo a stall cycle (i.e., stay on its current cell). There are other possibilities such as an evasive move or backtracking to avoid interference, but these lead to more substantial changes in the

scheduled droplet paths and are therefore not considered in this paper.

Let us denote two droplets by D_i and D_j, with the position of droplet D_i at time t given by $P_i(t)$. Let $N_i(t)$ be the set of directly adjacent neighbors of droplet D_i. The operator $\bar{k}(\bullet)$ is the set of pins that control the set of cells given by $\bullet$. Then the problem of two droplets moving concurrently can be formally stated as:

- D_i moves from $P_i(t)$ to $P_i(t+1)$
- D_j moves from $P_j(t)$ to $P_j(t+1)$

We are interested in the overlap of *pins* between sets of cells for the interference constraints, rather than the spatial locations of the cells. The latter are important for the fluidic constraints discussed in [20]. For the purpose of defining interference behavior, the system is completely determined by the positional states of the two droplets at times t and $t+1$. For droplet D_i, the positional states are characterized by the quartet ($P_i(t)$, $P_i(t+1)$, $N_i(t)$, $N_i(t+1)$) and for D_j, the pair ($P_j(t)$, $P_j(t+1)$, $N_j(t)$, $N_j(t+1)$). We consider $\bar{k}(\bullet)$ of all unordered pairs involving the following sets: $P_i(t)$, $P_i(t+1)$, $N_i(t)$, $N_i(t+1)$, $P_j(t)$, $P_j(t+1)$, $N_j(t)$, $N_j(t+1)$. Since $\binom{8}{2}=28$, there are 28 such pairs that may need to be mutually exclusive to prevent interference between the droplets. Pairs of cell sets that must be mutually exclusive for non-interference must be contained in this pool of unordered pairs because these eight sets include all cells currently occupied by droplets and all of their neighboring cells. Twenty-two pairs can be quickly removed from consideration, leaving only six pairs of sets that need to be closely examined to determine if their mutual exclusion is required for non-interference. For simplicity, the pin operator $\bar{k}(\bullet)$ is left implicit in the following discussion. Mutual exclusion always refers to the *pins* controlling the cells, and not the cells themselves.

Pair 1 $\{P_i(t), N_j(t)\}$: if $N_j(t)$ contains a cell that shares the same pin as $P_i(t)$, then D_j may be between $P_j(t)$ and $P_j(t+1)$ at time t. If this is not the case, D_j will not be able to move to $P_j(t+1)$ because it will no longer overlap with $P_j(t+1)$.

Pair 2 $\{P_i(t+1), N_j(t)\}$: if $N_j(t)$ contains a cell that shares the same pin as $P_i(t+1)$, D_j will not move properly at time $t+1$ unless $P_j(t+1)$ is the cell in $N_j(t)$ that shares the same pin as $P_i(t+1)$.

Pair 3 $\{P_i(t+1), N_j(t+1)\}$: if $N_j(t+1)$ contains a cell that shares the same pin as $P_i(t+1)$, then D_j will drift after moving to $P_j(t+1)$ so that it ends up between $P_j(t+1)$ and a cell that is an element of $N_j(t+1)$.

Pair 4 $\{N_i(t), P_j(t)\}$: if $N_i(t)$ contains a cell that shares the same pin as $P_j(t)$, then at time t, D_i will drift between $P_i(t)$ and the cell of interest in $N_i(t)$. D_i may no longer overlap with $P_j(t+1)$; if so, it will not be able to move to $P_j(t+1)$.

Pair 5 $\{N_i(t), P_j(t+1)\}$: if $N_i(t)$ contains a cell that shares the same pin as $P_j(t+1)$, D_i will not move properly at time $t+1$ unless $P_i(t+1)$ is the cell in $N_i(t)$ that shares the same pin as $P_j(t+1)$.

Pair 6 $\{N_i(t+1), P_j(t+1)\}$: if $N_i(t+1)$ contains a cell that shares the same pin as $P_j(t+1)$ then at time $t+1$, D_i will drift between $P_i(t+1)$ and the cell of interest in $N_i(t+1)$.

We have analytically confirmed that the control pins of these six pairs must be mutually exclusive to prevent interference between droplets D_i and D_j. These lead to the following necessary and sufficient interference constraints:

$$(1)\ \bar{k}\left(\{P_i(t)\}\right)\cap\bar{k}\left(N_j(t)\right)=\varnothing;\quad (2)\ \bar{k}\left(\{P_i(t+1)\}\right)\cap\bar{k}\left(N_j(t+1)\right)=\varnothing;$$
$$(3)\ \bar{k}\left(N_i(t)\right)\cap\bar{k}\left(\{P_j(t)\}\right)=\varnothing;\quad (4)\ \bar{k}\left(N_i(t+1)\right)\cap\bar{k}\left(\{P_j(t+1)\}\right)=\varnothing;$$
$$(5)\ \bar{k}\left(\{P_i(t+1)\}\right)\cap\bar{k}\left(N_j(t)-\{P_j(t+1)\}\right)=\varnothing;$$
$$(6)\ \bar{k}\left(\{P_j(t+1)\}\right)\cap\bar{k}\left(N_i(t)-\{P_i(t+1)\}\right)=\varnothing.$$

Moving one droplet and stalling the other is a special case that can be used when concurrent movement of two droplets leads to violation of the interference constraints. In this situation, $P_j=P_j(t)=P_j(t+1)$ and the interference constraints reduce to

$$(1)\ \bar{k}\left(\{P_i(t)\}\right)\cap\bar{k}\left(N_j\right)=\varnothing;\quad (2)\ \bar{k}\left(\{P_i(t+1)\}\right)\cap\bar{k}\left(N_j\right)=\varnothing;$$
$$(3)\ \bar{k}\left(N_i(t)\right)\cap\bar{k}\left(\{P_j\}\right)=\varnothing;\quad (4)\ \bar{k}\left(N_i(t+1)\right)\cap\bar{k}\left(\{P_j\}\right)=\varnothing.$$

Given k independent pins, our goal is to maximize the number of independent movements that a droplet can undertake from each position of the array while not interfering with another droplet on the same array. If interference results, some droplets can be forced to wait (stall cycle) while others move. If interference still occurs, then there is no safe way to transport the droplets on the same array along their desired paths unless the schedule is modified. In order to develop a useful, application-independent index that represents the independence of movement for two droplets on an array that can be easily extended to multiple droplets, we need a metric for comparison. If every cell has a dedicated control pin, there is no possibility of interference between droplets. Hence, only the fluidic constraints need to be considered.

We consider the case of one droplet moving while the other droplet waits. Let Φ be the set of all possible pin configurations using k pins for an $n\times m$ array. For a particular pin configuration $c\in\Phi$ using k-pins in our 2-droplet system, let $I_c(k,n,m)$ be the pin-constrained non-interference index (PCNI). It takes a value between 0 and 1 and equals the fraction of legal moves for two droplets (one moving, one waiting) on an $n\times m$ array with each cell having its own dedicated control pin that are still legal with pin layout $c\in\Phi$ and $k<n\times m$ pins, i.e.,

$$I_c(k,n,m)=\frac{number\ of\ legal\ moves\ in\ configuration\ c\ with\ k<n\times m\ pins}{number\ of\ legal\ moves\ with\ k=n\times m\ pins}$$

The interference and fluidic constraints discussed above can be used to determine $I_c(k,n,m)$ for a given pin layout. The computational complexity of this procedure is $O(n^2m^2)$. For example, consider the 3x4 array with the 9-pin layout shown in Figure 3(a). Using the interference and fluidic constraints, we determine that there are a total of 48 legal moves for the given array dimensions and pin layout. The reference pin layout, which provides full controllability with 12 independent pins and yields 148 legal moves, is shown in Figure 3(b). Therefore, the fraction of legal moves for the reference pin layout that are still legal for the proposed pin layout is 48/148 = 0.324. Two other layouts and their PCNIs are illustrated in Figures 3(c) and 3(d). Better layouts seem to loosely obey two principles: 1) Spread out the placement of pins that are used multiple times and 2) Place multiply-used pins on cells that have fewer neighbors (e.g., sides and corners).

For the case of two droplets moving concurrently, we use the same definition as before for the PCNI, except that a legal move is now characterized by a unique quartet, ($P_i(t)$, $P_i(t+1)$, $P_j(t)$, $P_j(t+1)$), that satisfies the fluidic and interference constraints. For example, for the same 3x4 array with the pin layout shown in Figure 3(a), there are a total of 88 legal moves. The reference pin layout, shown in Figure 3(b), yields 264 legal moves. Therefore, the fraction of legal moves for the reference pin layout that are still legal for the proposed pin layout is 88/264 = 0.333.

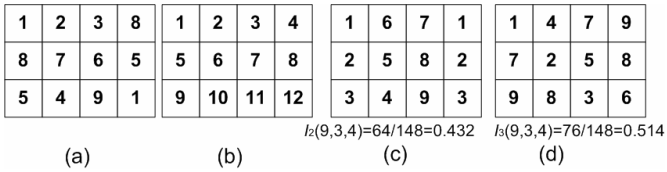

Figure 3. (a) 9-pin layout, (b) reference pin layout, (c) alternative 9-pin layout, and (d) second alternative 9-pin layout for a 3x4 array.

5. VIRTUAL PARTITIONING SCHEME

An alternative method of controlling multiple droplets on a single array is to "virtually" partition the array into regions. At any given time, partitions use non-overlapping sets of pins. Recall that regardless of size, a two-dimensional array needs a minimum of $k = 5$ pins to have full control of a single droplet when the diagonal adjacent effect is neglected. If there is a maximum of one droplet in each partition at all times, then interference is not possible.

With the partitioned array, the number of droplets that can be transported simultaneously *without* stall cycles is equal to the number of partitions since partitions do not share any control pins (i.e., no interference between partitions is possible). Fluidic constraints must be satisfied so that inadvertent mixing at partition boundaries does not occur.

As the number of droplets increases, the control bandwidth for an array based on the partitioned layout increases gradually with respect to the fixed $k = 5$, which is the minimum number of pins needed for a non-partition pin layout that yields full control of a single droplet regardless of array size. However, the *absence of interference* becomes more and more significant relative to the non-partitioned pin layout and usually outweighs the reduced flexibility incurred from the partitions. Moreover, another distinct advantage of the partitioned pin layout is that all droplets can move simultaneously since there is almost never a need for a droplet to wait. However, one disadvantage of a partitioned system of pins is the reduction in reconfigurability. We address dynamic rearrangement of the partitions in the next section.

5.1 Impact of Partitioning on PCNI

The 5x5 array shown in Figure 4(a) has a 10-pin layout. A cursory examination shows that even a single droplet will suffer from interference on this array. For example, any droplet in columns 2, 3, or 4 will be confined to its current column—horizontal movement is impossible. The problem is that the interior cells of the array are not surrounded by unique neighbors. To address this issue, we vertically flip the third and fourth columns and then swap the control pins of cells (4,2) and (4,3) with (2,2) and (2,3) respectively, as shown in Figure 4(b). Note that the first row and first column are referred to as (0,x) and (x,0) respectively.

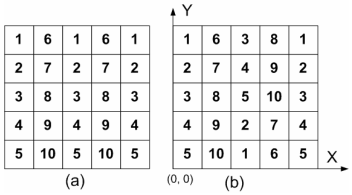

Figure 4. **(a) 10-pin layout, (b) another 10-pin layout for a 5x5 array.**

With this modified layout, every cell has a set of unique nearest neighbors in terms of control pins, allowing for unhindered movement of a single droplet. This new arrangement is characterized by a two-droplet one-move/one-wait PCNI of 0.2626. For most assays, we can divide the array into two partitions to accommodate two droplets such that they will never interfere.

Once the partitions are determined and the electrical connections between the electrodes and the external pins are laid out on the substrate (or the PCB), we have a hardwired platform. We envision that most chips will be used in a disposable manner such that it will run a set of pre-determined assays throughout its lifetime. A fixed partitioning scheme that accommodates the desired set of assays can be found prior to manufacturing and there is no need for partition reconfiguration. However, the effectiveness of a particular partitioning scheme may be reduced if a user maps other assay protocols onto the same partition configuration. A switch network can be used to dynamically reconfigure the interconnections between the k electrical signals and the $m \times n$ signals that drive the electrode array as shown in Figure 5(a). The control signals can either be derived from a computer-controlled setup, or the switch network and the control signals can be implemented using a field-programmable gate-array. These partitions can either be changed between sets of concurrent assays, or at appropriate "breakpoints" during assay execution. An example partition is shown in Figure 5(b). This partitioned array has a PCNI of 0.4041, a 53.8842% increase relative to the non-partitioned array in Figure 4(b).

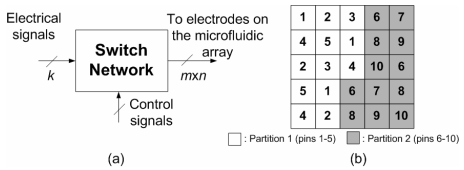

Figure 5. **(a) Dynamically-reconfigurable interconnection network; (b) two-partition layout for a 5x5 array.**

In general, if we partition an array such that at any time during an assay, at most one droplet occupies each partition, we can guarantee that the assay will be completed at the same throughput as the fully-addressable array with $k = n$ x m. However, computation of the PCNI is no different for partitioned arrays relative to non-partitioned arrays; the increases in PCNI observed for partitioned arrays do not involve adherence to the rule of at most one droplet per partition at all times.

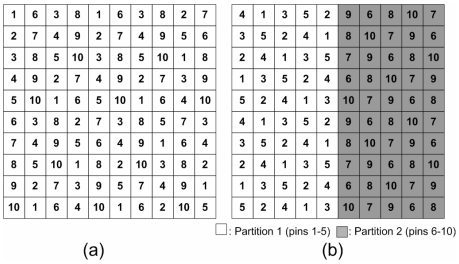

Figure 6. **(a) Non-partitioned and (b) two-partition 10-pin layout for a 10x10 array.**

Consider the non-partitioned 10x10 array with $k = 10$ shown in Figure 6(a). The non-interference index is 0.1467. If we instead divide the array into two partitions, still with $k = 10$, then one possible layout is shown in Figure 6(b). The non-interference index increases to 0.4565 for the 2-partition array, an increase of 211.18% relative to the non-partitioned array. In general, as the array size increases, and the number of pins and number of partitions remains constant, the PCNI for a partitioned array will increase while that of a non-partitioned array will decrease. The reasons for this are the following: (1) For a non-partitioned array, the possibilities for interference increase as array size increases and pins number remains the same, and (2) For a partitioned array, the partition size increases with the array size if k and the number of partitions are constant. Larger partitions mean that the proportion of movement pairs that violate fluidic constraints at the borders decreases, while interference is more rarely a concern for a partitioned array.

Figure 7(a) shows the same 10x10 array with the two partitions rearranged. The index is 0.4215, which is slightly less than the index value of 0.4565 obtained with the vertical-boundary partition configuration in Figure 6(b).

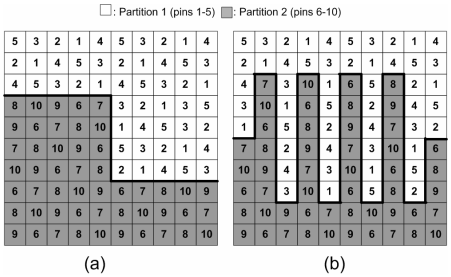

Figure 7. **Two-partition layouts for a 10x10 array with (a) medium boundary length, and (b) long boundary length.**

It is interesting to examine why the second partitioning scheme results in a lower PCNI. The boundary length between the partitions dictates the number of opportunities for fluidic interference (i.e., inadvertent mixing) between two droplets even when they satisfy the "rule" of at most one droplet per partition at any given time. The boundary length of the first partitioning scheme is 10 edges whereas the boundary length of the second is 14 edges. To illustrate this further, the example in Figure 7(b) also has two partitions for a 10x10 array with k = 10. The boundary length is 58. As expected, the PCNI drops significantly to 0.2478 with the large increase in boundary length, but it still represents a 68.92% increase relative to the non-partitioned array. These observations lead us to conclude that, to maximize the PCNI, the boundary length between partitions should be kept to the minimum possible for a given assay.

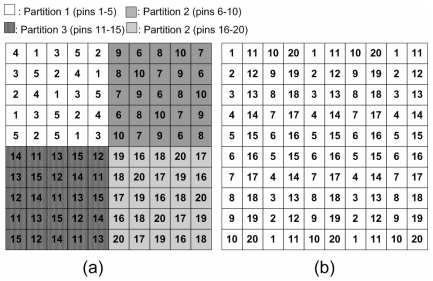

Figure 8. **Partitioned pin layout for a 10x10 array with k = 20 and 4 partitions; (b) non-partitioned pin layout for a 10x10 array.**

To illustrate the use of multiple partitions, consider the array pin layout with k = 20 and 4 partitions, as shown in Figure 8(a). The two droplet PCNI is 0.7331 relative to the non-partitioned array shown in Figure 8(b), which yields an index of 0.6772. It is important to note that since the PCNI reported here is only computed for two droplets simultaneously on the array, the advantages of the 4-partition layout in Figure 8(a) are not being fully exploited. Whereas four droplets maintained in unique partitions would have no potential for interference and therefore the four-droplet PCNI will only drop slightly for the partitioned array relative to the two-droplet PCNI, the four-droplet PCNI will drop precipitously for the non-partitioned array. It is remarkable that even if we ignore this obvious advantage, the PCNI of the partitioned array is still 8.25% higher than that of the non-partitioned array. Even though the virtual partitions are not considered in the computation of the PCNI, the virtual partitioning scheme still leads to significantly higher indices relative to non-partitioned arrays. Therefore, it is generally advantageous to partition the array even if the assays of interest use the array in a random fashion, i.e., with no regard to the partitions.

5.2 Evaluation Example: Multiplexed Bioassays

To show how the proposed virtual partitioning method can be used for pin-constrained microfluidic biochips, we apply it to a multiplexed biochemical assay consisting of a glucose assay and a lactate assay based on colorimetric enzymatic reactions, which have been demonstrated recently [3].

The digital microfluidic biochip contains a 15×15 microfluidic array, as shown in Figure 9. The schedule for the set of bioassays, if a fully-addressable array with 225 control pins is available, is listed in Table 1; one iteration of the multiplexed assays takes 25.8 seconds. The movement of droplets is controlled using a 50 V actuation voltage with a switching frequency of 16 Hz. A depiction of the droplet paths for multiplexed glucose and lactase assays is illustrated in Figure 9.

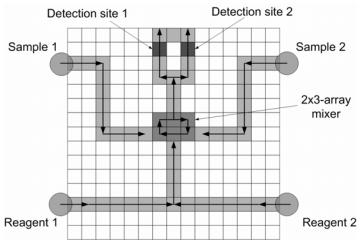

Figure 9. **15×15 array used for multiplexed bioassays.**

Table 1. **Bioassay schedule for a full-addressable array.**

Step/Time Elapsed (s)	Operation
Step 1 / 0	Sample (S) 2 and reagent (R) 2 start to move towards the mixer.
Step 2 / 0.8	S2 and R2 begin to mix together and turn around in the 2×3-array mixer.
Step 3 / 6.0	S1 and R1 start to move towards the mixer. S2 and R2 continue to mix.
Step 4 / 6.8	S2 and R2 finish the mixing and product (P) 2 leaves the mixer to optical detection location 2. S1 and R1 begin to mix in the mixer.
Step 5 / 12.8	S1 and R1 finish the mixing and P1 leaves the mixer to the optical detection location 1. P2 continues the absorbance detection.
Step 6 / 19.8	P2 finishes optical detection & leaves the array to waste reservoir. P1 continues the absorbance detection.
Step 7 / 25.8	P1 finishes optical detection and leaves the array to the waste reservoir. One procedure of the multiplexed bioassays ends.

As with most assays, partitioning of the pin layout is effective in reducing the input bandwidth while maintaining the same throughput. Five partitions are satisfactory in preventing interference between multiple droplets on the array, as shown in Figure 10. Since only five control pins are necessary for full control of a single droplet within each partition, only 25 out of the possible 225 control pins are necessary, i.e., 11.11%. This represents a significant reduction in input bandwidth without sacrificing throughput. Note that the mixing region (i.e., Partition 2) is arranged such that as soon as Sample and Reagent enter the mixer, they merge to form one droplet so that there is no need to worry about multiple droplets in the mixer and the potential interference, precluding the need for a dedicated mixing region.

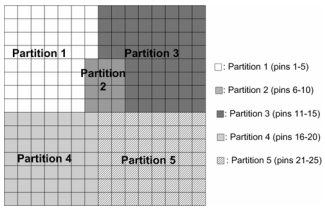

Figure 10. **Partitioned 15×15 microfluidic array.**

If the 15x15 array uses 25 control pins without partitioning, throughput will likely be greatly reduced if the assay can be completed at all. To illustrate this, let us examine a similar assay on a smaller 5x5 array (Figure 11) that has a fully-addressable layout. The assay schedule is also shown in the Figure 11.

Suppose we are constrained to only having 10 pins. The layout shown in Figure 12(a) is one possible design, and it has a non-interference index of 0.169811. The assay takes almost twice as long with the pin-constrained layout without partitioning, as illustrated by the revised schedule in Figure 12. On the other hand,

partitioning can be used to remove interference. The array shown in Figure 12(b) has two partitions and only uses 9 pins. The throughput of this pin layout is the same as that of Figure 11.

Time	Action	P_i	P_j	P_k
1	Dispense	(4,1)	(4,5)	-
2	Move	(4,2)	(4,4)	-
3	Merge	(4,3)	(4,3)	-
4	Mix	(4,4)	(4,4)	-
5	Mix	(3,4)	(3,4)	-
6	Mix	(3,3)	(3,3)	-
7	Mix, Dispense	(3,2)	(3,2)	(4,5)
8	Split, Move	(2,2)	(4,2)	(4,4)
9	Detect, Merge	(1,2)	(4,3)	(4,3)
10	Mix		(4,2)	(4,2)
11	Mix		(3,2)	(3,2)
12	Mix		(3,3)	(3,3)
13	Mix		(3,4)	(3,4)
14	Split		(2,4)	(4,4)
15	Detect		(1,4)	(5,4)
16	Dispose			into waste

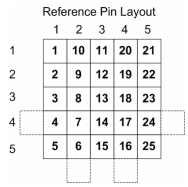

Figure 11. **5x5 array with a fully addressable layout, and the corresponding assay schedule.**

Time	Action	Pins Active	P_i	P_j	P_k
1	Dispense	5,10	(4,1)	(4,5)	-
2	Stall D_i, Move D_j	4,10	(4,1)	(4,4)/(3,4)	-
3	Move D_i, Stall D_j	2,4	(4,2)	(4,4)	-
4	Merge	4	(4,3)	(4,3)	-
5	Mix	4	(4,4)	(4,4)	-
6	Mix	10	(3,4)	(3,4)	-
7	Mix	6	(3,3)	(3,3)	-
8	Mix	7	(3,2)	(3,2)	-
9	Dispense D_k	5,7	(3,2)	(3,2)	(4,5)
10	Move D_k	4,7	(3,2)	(3,2)	(4,4)
11	Split D_{ij}	1,2,4	(2,2)	(4,2)	(4,4)
12	Detect, Merge	3	(1,2)	(4,3)	(4,3)

We cannot move D_{jk} since D_i needs to stay on the detector.
Suppose detection takes 10 time steps.

23	Mix, Dispose D_{ij}	2	-	(4,2)	(4,2)
24	Mix	7	-	(3,2)	(3,2)
25	Mix	6	-	(3,3)	(3,3)
26	Mix	10	-	(3,4)	(3,4)
27	Split	4,8	-	(2,4)	(4,4)(5,4)
28	Move	4,7	-	(1,3) /(1,4)	(4,4)
29	Move	7,8	-	(1,4)/ (2,4)	(5,4)

At least two extra time steps are added to the second detection because the drift interference delays initiation of the detection step.

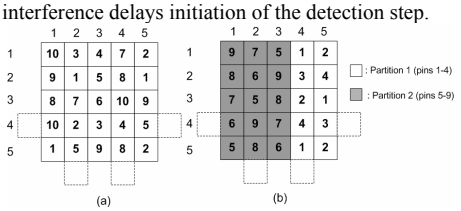

Figure 12. **(a) Non-partitioned 10-pin layout (PCNI = 16.9811%) and the corresponding schedule; (b) partitioned 9-pin layout.**

Biological samples are sensitive to the environment, and it is difficult to maintain an optimal environment for them on chip. It is therefore desirable to minimize the time samples spend on chip before assay results are obtained. Increased throughout also improves operational reliability. If there are too many stalls, high voltages will have to be maintained on some electrodes, which will accelerate insulator degradation and dielectric breakdown, reducing the number of assays that can be performed on a chip during its lifetime. It is also important to note that for many assays, using a pin-constrained, non-partitioned array does not simply reduce throughput—it actually causes droplet deadlock such that assays cannot be completed even with an infinite number of stalls.

6. CONCLUSION

In this paper, we have presented a design method for pin-constrained digital microfluidic biochips. We first formulated the problem of determining the minimum number of control pins for full control of a single droplet. The interference problem for multiple droplets on a pin-constrained biochip has also been investigated. A new method called virtual partitioning has been proposed to reduce or remove interference in pin-constrained biochips. The real-life example of a set of multiplexed bioassays has been used to evaluate the effectiveness of the proposed method. By dramatically reducing the number of control pins with minimal impact on assay throughput, the proposed design method is expected to reduce cost and lead to the miniaturization of mixed-technology disposable biomedical devices for the emerging healthcare market.

7. REFERENCES

[1] E. Verpoorte and N.F. De Rooij, "Microfluidics meets MEMS", *Proceedings of the IEEE*, vol. 91, pp. 930-953, 2003.

[2] T.H. Schulte et al., "Microfluidic technologies in clinical diagnostics", *Clinica Chimica Acta*, vol. 321, pp. 1-10, 2002.

[3] V. Srinivasan et al., "An integrated digital microfluidic lab-on-a-chip for clinical diagnostics on human physiological fluids," *Lab on a Chip*, pp. 310-315, 2004.

[4] Infineon Electronic DNA Chip, http://www.infineon.com

[5] Nanogen NanoChip®, http://www.nanogen.com

[6] M.G. Pollack et al., "Electrowetting-based actuation of liquid droplets for microfluidic applications", *Applied Physics Letters*, vol. 77, pp. 1725-1726, 2000.

[7] S.K. Cho et al., "Toward digital microfluidic circuits: creating, transporting, cutting and merging liquid droplets by electrowetting-based actuation", *Proc. IEEE MEMS Conf.*, pp. 32-52. 2002.

[8] T. Mukherjee and G.K. Fedder, "Design methodology for mixed-domain systems-on-a-chip [MEMS design]", *Proc. IEEE VLSI System Level Design*, pp. 96 - 101, 1998.

[9] International Technology Roadmap for Semiconductors (ITRS), http://public.itrs.net/Files/2003ITRS/Home2003.htm.

[10] F. Su and K. Chakrabarty, "Architectural-level synthesis of digital microfluidics-based biochips", *Proc. IEEE Intl. Conf. on CAD*, pp. 223-228, 2004.

[11] F. Su and K. Chakrabarty, "Design of fault-tolerant and dynamically-reconfigurable microfluidic biochips", *Proc. DATE Conference*, pp.1202-1207, 2005.

[12] J. Gong, and C.J. Kim, "Two-dimensional digital microfluidic system by multi-layer printed circuit board," *Proc. of IEEE MEMS 2005*, pp. 726-729, 2005.

[13] M.G. Pollack, *Electrowetting-Based Microactuation of Droplets for Digital Microfluidics*, PhD thesis, Duke University. 2001.

[14] P.Y. Paik et al., "Rapid droplet mixers for digital microfluidic systems", *Lab on a Chip*, vol. 3, pp. 253-259, 2003.

[15] P.Y. Paik et al., "Coplanar digital microfluidics using standard printed circuit board processes", *Proc. Intl. Conf. on MicroTAS*, pp. 566-568, 2005.

[16] F. Su and K. Chakrabarty, "Unified high-level synthesis and module placement for defect-tolerant microfluidic biochips", *Proc. IEEE/ACM DAC*, pp. 825-830, 2005.

[17] S.K. Fan et al., "Manipulation of multiple droplets on N×M grid by cross-reference EWOD driving scheme and pressure-contact packaging", *Proc. IEEE MEMS Conf.*, pp. 694-697, 2003.

[18] J. Gross and J. Yellen, *Graph Theory and its Applications*, Boca Raton, FL: CRC Press, 1999.

[19] C.H. Papadimitriou, *Computational Complexity*, Reading, MA: Addison Wesley, 1993.

[20] F. Su, W. Hwang, and K. Chakrabarty, "Droplet routing in the synthesis of digital microfluidic biochips", *Proc. DATE Conference*, 2006.